ELSEVIER

Thermochimica Acta 260 (1995) 125–136

thermochimica acta

Direct sulfation reaction of SO_2 with calcium carbonate

Qin Zhong

Chemical Engineering Institute, Nanjing University of Science and Technology, 210094 Nanjing, People's Republic of China

Received 10 October 1994; accepted 14 January 1995

Abstract

The direct sulfation reaction of SO_2 with $CaCO_3$ has been investigated by thermogravimetry (TG) under the condition that the $CaCO_3$ does not decompose to CaO prior to sulfation by controlling CO_2 partial pressure. The direct sulfation process can be described by using a shrinking-core model for constant particle size. The model shows that the reaction rate and the diffusion rate of SO_2 through the product layer are equally important. Temperature effects can be correlated by the activation energy of 35.9 kJ mol^{-1} for the sulfation reaction and 66.5 kJ mol^{-1} for the product layer diffusion. The sulfation reaction is found to be first order with respect to SO_2. With larger pore volume and surface area of limestone samples, the sorbents have a stronger reactivity of SO_2 removal. A 70% $CaCO_3$ conversion can be achieved in 10 min at 800°C and 2000 ppm SO_2.

Keywords: Calcium carbonate; Direct sulfation; Model

1. Introduction

The conventional method for removing sulfur dioxide from coal combustion involves decomposing $CaCO_3$ to CaO, which subsequently combines with gaseous SO_2 to form calcium sulfate

$$CaCO_3(s) \longrightarrow CaO(s) + CO_2(g) \quad (1)$$

$$CaO(s) + SO_2(g) + 1/2O_2(g) \longrightarrow CaSO_4(s) \quad (2)$$

At temperatures below the decomposition temperature of $CaCO_3$, the direct reaction of SO_2 with $CaCO_3$ in the presence of O_2 is believed to occur [1]

$$CaCO_3(s) + SO_2(g) + 1/2O_2(g) \longrightarrow CaSO_4(s) + CO_2(g) \quad (3)$$

SSDI 0040-6031(95)02258-9

However, the following reactions are also reported [2]

$$CaCO_3(s) + SO_2(g) \xrightarrow{1} CaSO_3(s) + CO_2(g) \xrightarrow[+1/2O_2]{2} CaSO_4(s) \quad (4)$$

The direct reaction differs from reactions (1) and (2) by avoidance of formation of CaO crystals, and generation of CO_2 at the reaction interface. Because of these differences, one would expect differences in relationships between sulfation rate and conversion.

Bjerle and Ye [3] analyzed with X-ray diffraction the samples prepared in an entrained flow reactor at 1000°C, and found that some $CaCO_3$ of the calcined samples was left unconverted, but that no $CaCO_3$ was present in the sulfatized samples. They thought that SO_2 may react directly with $CaCO_3$ to $CaSO_4$.

Snow et al. [1] explored the direct sulfation reaction using TG. They found that the direct sulfation of $CaCO_3$ had a higher conversion than the sulfation of precalcined limestone, and that the diffusion resistance through the product layer was significantly smaller than that encountered in the usual sulfation of CaO. Based on Snow's work, Hajaligol et al. [4] extended the research. They confirmed that direct sulfation of $CaCO_3$ showed higher conversion in isothermal sulfation, due to formation of a more porous calcium sulfate layer, and found that the porosity of the samples increased with the rate of CO_2 generation.

Spartinos and Vayenas [5] performed kinetic studies of the direct sulfation in a tubular isothermal reactor. They found that the diffusion of SO_2 through the product $CaSO_4$ layer was rate-limiting, and the effective diffusivity of SO_2 in the limestone sulfation was two to three orders of magnitude higher than in the sulfation of precalcined limestone.

Van Houte et al. [2] investigated the direct sulfation reaction at low temperature in a fixed bed reactor. In their study, the sulfite ($CaSO_3$) was also a stable product. They observed that below 650°C, reagent-grade $CaCO_3$ (1–15 μm) impregnated with $CaCl_2$ showed complete sulfation, and concluded that the oxidation of sulfite was rate-limiting. Unimpregnated $CaCO_3$ sulfated at slower rates, initially zero-order with respect to SO_2 and first-order with respect to O_2. Based on detailed examination of SEM photomicrographs, they observed that the calcium sulfate layer formed during the direct sulfation was porous.

The objective of this study was to characterize experimentally the reactivity of SO_2 with limestones. A TG reactor was used to investigate the effects of limestone type, reaction time, temperature, particle size and SO_2 partial pressure on the conversion of $CaCO_3$ to $CaSO_4$. A theoretical model was developed and fitted to the experimental data.

2. Experimental

2.1. Test sorbent

Three specimens that were confirmed as limestones by X-ray diffraction were used in most of the study. A summary of the chemical and physical properties of these materials is presented in Table 1.

Table 1
Chemical (wt%) and physical properties of the samples

Limestone	$CaCO_3$	SiO_2	Al_2O_3	Fe_2O_3	MgO	K_2O	Na_2O	S	BET surface/$m^2 g^{-1}$
Forsby	95.60	0.26	0.30	0.23	0.88	0.01	0.09	0.11	10.3
Ignaberga	82.80	12.40	0.89	0.66	0.35	0.17	0.11	0.03	10.3
Limhamn	89.30	7.37	0.23	0.28	0.95	0.02	0.06	0.04	12.0

2.2. TG measurements

The TG apparatus used in the study was a Cahn-2000 electrobalance with a sample basket made of a fine Pt-net. A schematic diagram of the TG system has been published elsewhere [6]. To prepare the sample, the basket was dipped in a slurry containing 10–15 wt% of stone; about 5 mg of solid particles adhered to the basket. The basket was then dried under IR radiation in order to form a very thin layer of sample.

For establishing the reaction condition, the maximum temperature that can be reached without limestone decomposition was determined. Fig. 1 shows the decomposition temperature of Forsby limestone versus CO_2 equilibrium partial pressure at 1 bar. Up to 650°C in a gas stream of N_2, Forsby limestone does not decompose. Below 810°C, 10% CO_2 concentration in the gas phase is sufficient to prevent decomposition.

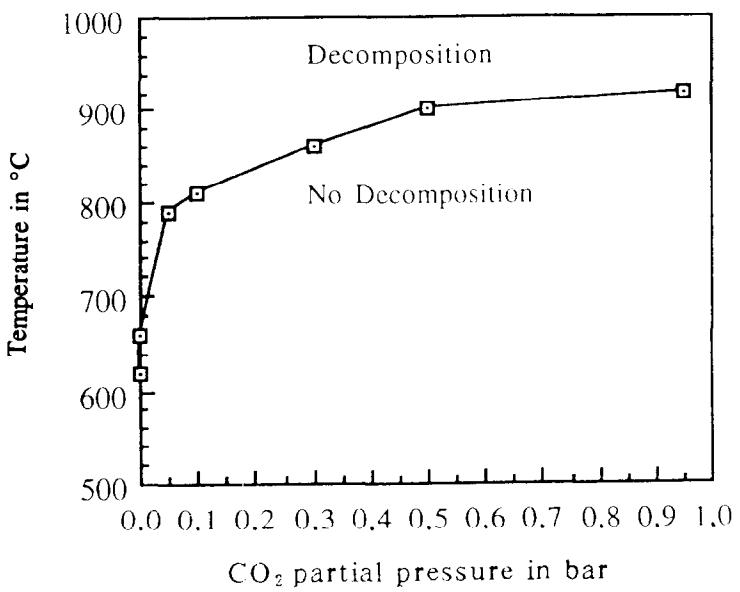

Fig. 1. The effect of CO_2 partial pressure on $CaCO_3$ decomposition temperature for Forsby limestone at 1 bar.

For the 95% CO_2 mixture, the decomposition temperature is about 920°C. The limestone sulfation can therefore be explored under the condition that the limestone does not decompose to CaO prior to sulfation by controlling CO_2 partial pressure.

The limestone sulfation procedure consisted of heating a sample at 60–70°C min^{-1} to the desired temperature, establishing isothermal conditions with the gas stream of 70% CO_2, 10% O_2 and 20% N_2, and then adding SO_2 in a concentration of 1000–5000 ppm, at a total pressure of 1 bar. The isothermal reaction temperature was varied from 500 to 800°C.

2.3. Grinding test

Finer particles were obtained by grinding limestone slurry in a small bead mill. The particle distribution of limestone slurry was measured by means of a sedigraph. For Forsby limestone, the mean particle sizes of 7-h-ground and unground samples are 4.0 μm and 5.4 μm, respectivley.

2.4. BET measurement

Both the BET surface and pore-size distribution measurements were conducted in a Cahn 2000 electrobalance-based system. In the BET method, nitrogen was used as the adsorption gas. From the adsorption/desorption isotherm, the pore size distribution can be calculated.

3. Results and discussion

3.1. Kinetics of direct sulfation

The usual way to assess the rate of reaction by the isothermal method is to measure the mass change (in this case an increase) as a function of time. Every TG curve was transferred to a $CaCO_3$ conversion versus time relationship, and the conversion data were corrected with the purity of $CaCO_3$. The conversion of $CaCO_3$ to $CaSO_4$ was investigated with Forsby limestone as a function of time, temperature, SO_2 partial pressure and particle size, as shown in Figs. 2–4.

Fig. 2 shows that the overall rate of $CaCO_3$ sulfation is strongly influenced by reaction time and temperature in the region 500–800°C. The rate is high in the initial stage of exposure, and then decreases gradually as the sulfation proceeds. The initial rapid reaction results from the higher surface area of unsulfated $CaCO_3$, acting in combination with rapid intrinsic kinetics. The rate decrease is due both to the surface area loss and to the build-up of a continuously growing product $CaSO_4$ layer on the surface of unreacted $CaCO_3$. Fig. 2 shows that at a fixed reaction time, $CaCO_3$ conversion increases with increasing temperature. The sulfation rate is rather slow at 500°C.

The effect of SO_2 partial pressure on the $CaCO_3$ sulfation rate was investigated in the region 1000–5000 ppm SO_2 and at 800°C, as shown in Fig. 3. The curves show that the

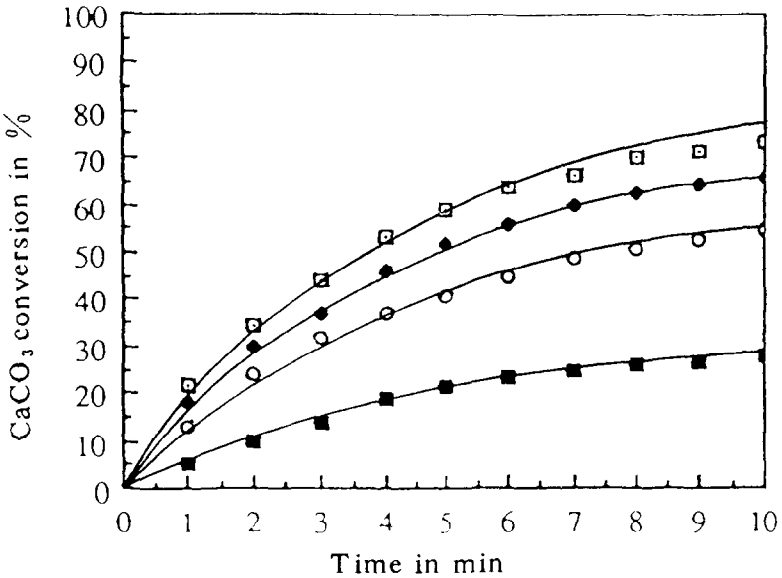

Fig. 2. The effect of reaction time and temperature on $CaCO_3$ conversion for Forsby limestone at 2000 ppm SO_2 and 500–800°C: ■, 500°C, exp.; ○, 600°C, exp.; ◆, 700°C, exp.; ⊡ 800°C, exp.; —, model.

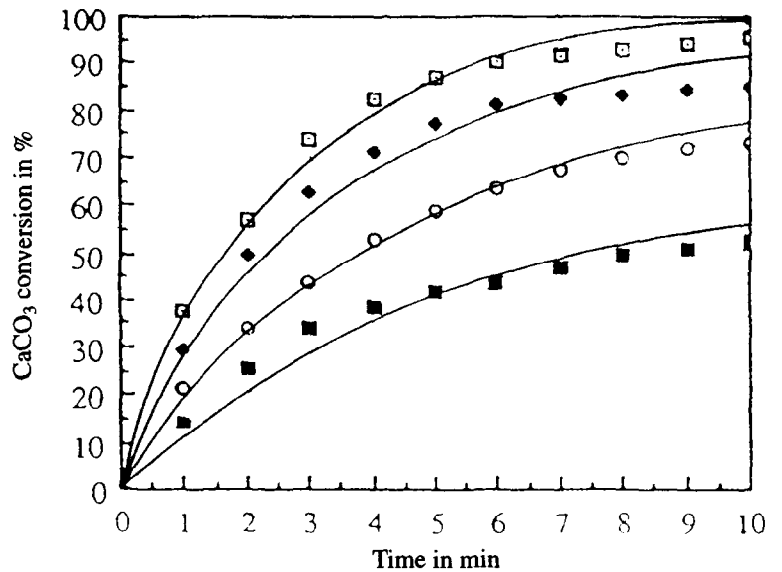

Fig. 3. The effect of SO_2 partial pressure on $CaCO_3$ conversion for Forsby limestone at 800°C and 1000–5000 ppm SO_2: ■, 1000 ppm SO_2, exp.; ○, 2000 ppm SO_2, exp.; ◆, 3500 ppm SO_2, exp.; ⊡ , 5000 ppm SO_2, exp.; —model.

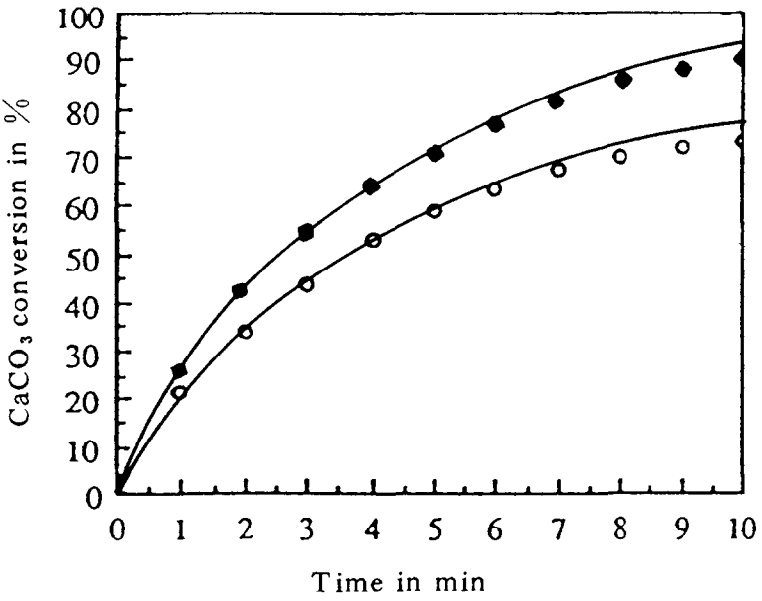

Fig. 4. The effect of particle size on $CaCO_3$ conversion for Forsby limestone at 800°C and 2000 ppm SO_2; ○, unground; ◆, ground for 7 h; —, model.

sulfation rate clearly increases as SO_2 partial pressure increases. The sulfation reaction with respect to SO_2 is found to be first order, as analysed in the model. The diffusion rates of SO_2 through the gas film and product layer increase with increasing SO_2 partial pressure, resulting in a positive effect on the sulfation rate.

Fig. 4 shows that the sulfation rate of ground sample is faster than that of unground sample, because ground samples have smaller diffusion resistances of SO_2 through the gas film and the $CaSO_4$ layer, and have larger cumulative pore volume and surface area, as shown in Figs. 5 and 6.

Fig. 7 shows the reactivity comparisons of three limestone samples at 800°C and 2000 ppm SO_2. Among the three samples, Ignaberga and Forsby exhibit the largest and the smallest reactivity, respectively. More than 70% $CaCO_3$ conversion efficiency can be reached in less then 10 min. The reactivity differences are mainly attributed to their original micro structures, as shown in Figs. 8 and 9.

3.2. Direct sulfation model

According to the above results, it is clear that the overall rate of $CaCO_3$ sulfation is dependent on time, temperature, SO_2 concentration, particle size and micro structure. In the literature, mathematical models of various degrees of complexity and sophistication have been proposed to describe the process of $CaCO_3$ sulfation [5, 7, 8], but these models require many parameters that are not available at present. Based on detailed examination of SEM photographs of sulfated samples, Hajaligol et al. [4] thought that

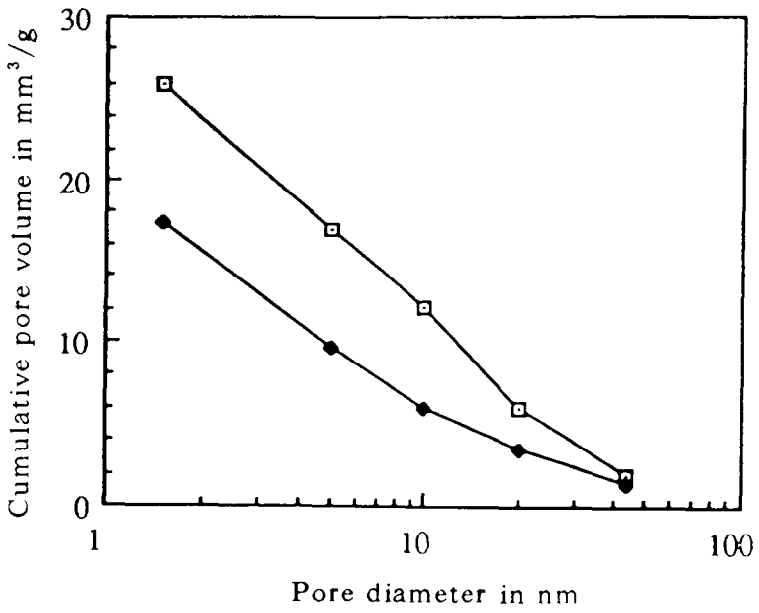

Fig. 5. The effect of sample grinding on pore volume distribution for Forsby limestone: ◆, unground; ⊡, ground for 7 h.

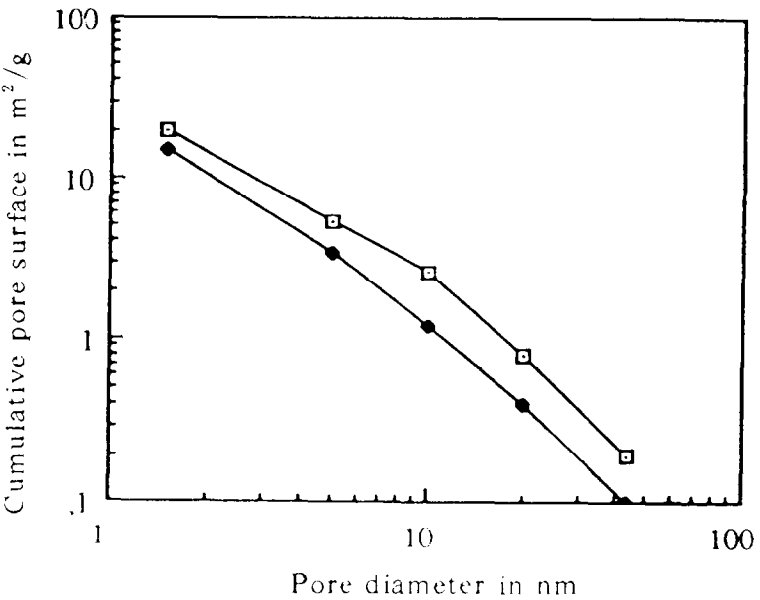

Fig. 6. The effect of sample grinding on pore surface area distribution for Forsby limestone: ◆, unground; ⊡, ground for 7 h.

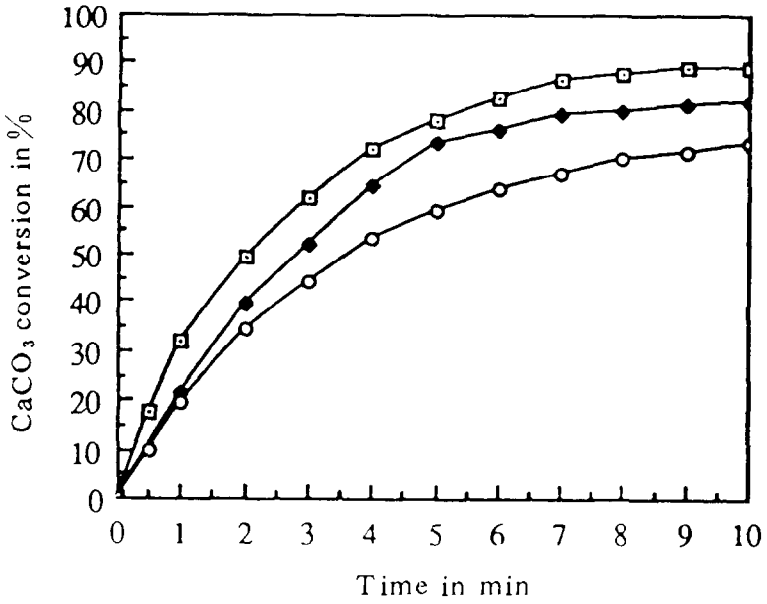

Fig. 7. The relativity comparisons of three limestone samples at 800°C and 2000 ppm SO_2: ○, Forsby; ◆, Limhamn; ⊡, Ignaberga.

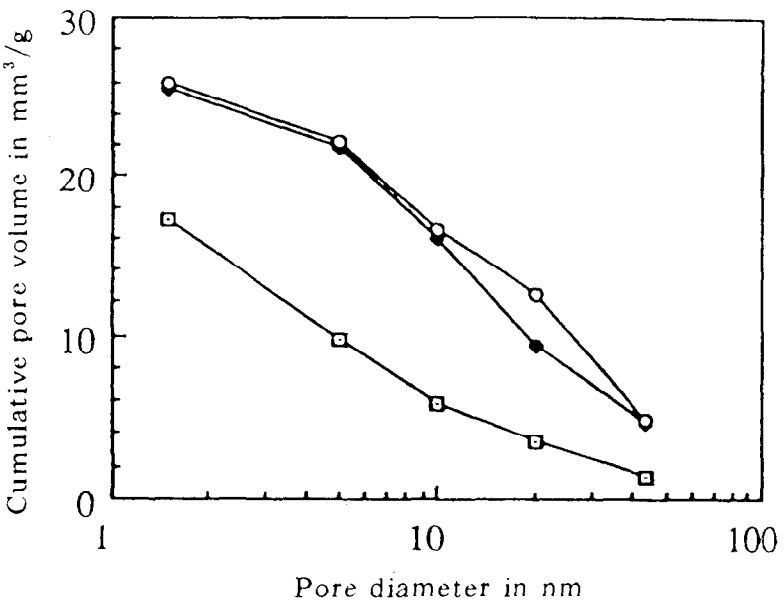

Fig. 8. The pore volume distributions of three tested limstone samples: ⊡, Forsby; ◆, Limhamn; ○, Ignaberga.

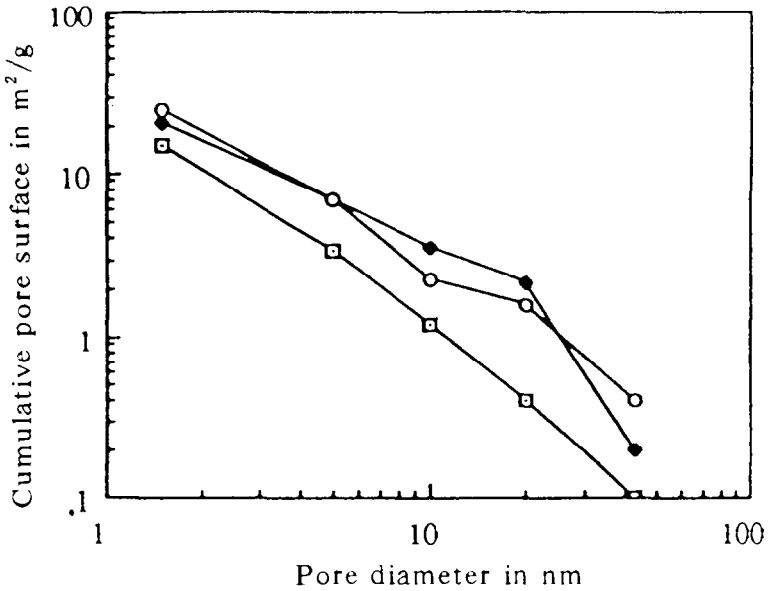

Fig. 9. The pore surface area distributions of three tested limestone samples: ⊡, Forsby; ◆, Limhamn; ○, Ignaberga.

the direct sulfation can be described by using a shrinking unreacted core model. In this study, the shrinking core model for spherical particles of constant size was used to simulate the sulfation process. The basic assumption of the model is that the mass transfer rate of SO_2 through the gas film (N_{SO_2} in kmol s^{-1}) equals the mass transfer rate of SO_2 through the product layer (N'_{SO_2} in kmol s^{-1}), and equals the reaction rate of SO_2 at the interface ($-r_{SO_2} S_i$ in kmol s^{-1}). N_{SO_2}, N'_{SO_2} and $-r_{SO_2}$ may be expressed as

$$N_{SO_2} = 4\pi R^2 k_g (C_g - C_s) \tag{5}$$

$$N'_{SO_2} = 4\pi r^2 D_e \frac{dC_{SO_2}}{dt} \tag{6}$$

$$-r_{SO_2} = k_s C_i^n = k_s C_i \tag{7}$$

where C_g and C_s as well as C_i are SO_2 concentrations (kmol m^{-3}) in the gas phase and at the gas–solid interface and reaction interface, respectively. D_e is the effecitve diffusivity of product layer (m^2 s^{-1}), k_g ($\approx D_{SO_2}/R$) is the mass transfer coefficient of the gas phase (m s^{-1}), k_s is a rate constant of the intrinsic reaction (m s^{-1}), and n is the reaction order ($n = 1$). R and r are the radii of initial and unreacted $CaCO_3$ particles, respectively. Assuming a steady state of mass trasfer in the product layer and that D_e is only a function of temperature, integration of Eq. (6) yields

$$N'_{SO_2} = 4\pi D_e \frac{C_s - C_i}{\frac{1}{r} - \frac{1}{R}} \tag{8}$$

According to the basic assumption

$$N_{SO_2} = N'_{SO_2} = -r_{SO_2} S_i = \frac{(C_g - C_s) + (C_s - C_i) + C_i}{\frac{1}{4\pi R^2 k_g} + \frac{1}{4\pi D_e}\left(\frac{1}{r} - \frac{1}{R}\right) + \frac{1}{4\pi r^2 k_s}} \tag{9}$$

N_{SO_2} can also be expressed as

$$N_{SO_2} = -\frac{dn_{SO_2}}{dt} = -\frac{dn_{CaCO_3}}{dt} = n_{CaCO_3,0}\frac{dX}{dt} = \frac{4}{3}\pi R^3 \rho \frac{dX}{dt} \tag{10}$$

where X is the conversion of $CaCO_3$, and ρ is the density of $CaCO_3$ (27 k mol m^{-3}). For spherical particles

$$X = 1 - \left(\frac{r}{R}\right)^3$$

Because of excess gas flow in the TG reactor, the SO_2 concentration of the gas phase is almost constant, and equals the initial SO_2 concentration ($C_g = C_0$). Using Eqs. (9) and (10), we obtain

$$\frac{dX}{dt} = \frac{k_0}{\frac{1}{D_{SO_2}} + \frac{(1-X)^{-1/3} - 1}{D_e} + \frac{(1-X)^{-2/3}}{Rk_s}} \tag{11}$$

where k_0 ($= 3C_0/\rho R^2$) is constant (m^2). Eq. (11) is the final model equation, and can be numerically solved. The gas phase diffusivity (D_{SO_2}) was calculated using the Chapman–Enskog formula [9] and is listed in Table 2. D_e and k_s were estimated for each temperature by fitting the model calculations to the experimental X–t data with a least-squares method, and results are listed in Table 2.

Figs. 2–4 show the comparisons of the experimental data and sulfation model predictions. This model can predict sufficiently well the effects of time, temperature, SO_2 partial pressure and particle size on the conversion of $CaCO_3$ to $CaSO_4$. Arrhenius plots of the rate constant and product layer diffusivity had been made, respectively, as shown in Fig. 10. The reaction activation energy from the slope of the straight line is estimated as 35.9 kJ mol^{-1}, and the diffusion activation energy as 66.5 kJ mol^{-1}. This result indicates that temperature has a stronger effect on the product layer diffusion, and that the diffusion process is limited by some kind of a high

Table 2
Model parameters

T/K	$D_{SO_2} \times 10^{-6}$ m^2 s^{-1}	$D_e \times 10^{-10}$ m^2 s^{-1}	$k_s \times 10^{-3}$ m s^{-1}
733	48.7	0.8	1.0
873	63.0	4.0	3.3
973	76.1	8.0	4.2
1073	90.2	15.0	4.9

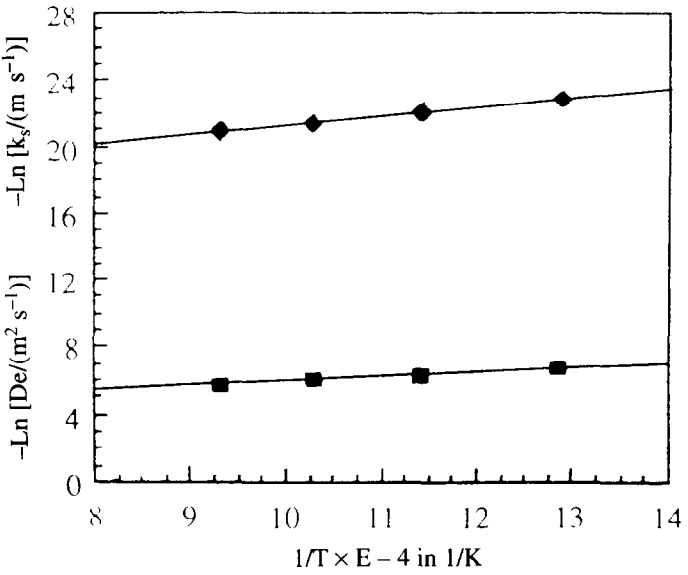

Fig. 10. Arrhenius plot for evaluation of activation energy for Forsby limestone at 500–800°C and 1000–2000 ppm SO_2: ◆, ln k_s; ■, ln D_e.

activation energy solid-state diffusion process. Similar results were obtained by Hajaligol et al. [4].

4. Conclusions

When CO_2 partial pressure exceeds the equilibrium partial pressure of $CaCO_3$, $CaCO_3$ cannot decompose. Therefore, the isothermal kinetics of direct sulfation of $CaCO_3$ could be studied in TG by controlling CO_2 partial pressure.

The $CaCO_3$ sulfation process can be described by using a shrinking-core model. The model calculation results show that the reaction rate and the diffusion rate of SO_2 through the product layer are equally important. Temperature effects can be correlated by the activation energy of 35.9 kJ mol^{-1} for the sulfation reaction and 66.5 kJ mol^{-1} for the product layer diffusion. The sulfation reaction is found to be first order with respect to SO_2. The reduction of particle size can enhance the sulfation process rate. A larger pore volume and surface area of limestone samples predict that these sorbents have a stronger reactivity of SO_2 removal. In the three tested samples, Ignaberga limestone shows the highest reactivity. A 70% $CaCO_3$ conversion can be achieved in 10 min at 800°C and 2000 ppm SO_2.

Acknowledgments

This work has been supported by the Swedish Energy Administration and the State Education Commission of China to which the author is grateful. The author is also

grateful to Professor Dr. Ingemar Bjerle of Swedish Lund University for his invaluable support and scientific guidance.

References

[1] M.J. Snow, J.P. Longwell and A.F. Sarofim, Ind. Eng. Chem. Res., 27 (1988) 268.
[2] G. van Houte, L. Rodrique, M. Genet and B. Delmon, Environ. Sci. Technol., 15 (1981) 327.
[3] I. Bjerle and Z. Ye, Chem. Eng. Technol., 14 (1991) 357.
[4] M.R. Hajaligol, J.P. Longwell and A.F. Sarofirm, Ind. Eng. Chem. Res., 27 (1988) 2203.
[5] D. Spartinos and C. Vayenas, Chem. Eng. Process., 30 (1991) 94.
[6] I. Bjerle, F. Xu and Z. Ye, Chem. Eng. Technol., 15 (1992) 151.
[7] P.A. Ramachandran and L.K. Doraiswamy, AIChE J., 28 (1982) 881.
[8] M. Sahimi, G.R. Gavalas and T.T. Tsotsis, Chem. Eng. Sci., 45 (1990) 1443.
[9] J.M. Smith, Chemical Engineering Kinetics, McGraw-Hill, New York, 3rd edn., 1981.